cells for 2 h, followed by a 72-h incubation. The cytotoxicity of the free THP was not affected by preincubation conditions at various pH values (not shown), whereas preincubation of PHPMA-hyd-THP at pH 5.5 greatly enhanced its cytotoxicity (Fig. 3B). This result suggests that the release of free THP from PHPMA-hyd-THP is critical for its cytotoxicity.

We also investigated the cytotoxicity of PHPMA-hyd-THP at different pH values (pH 7.4, 6.9, and 6.5), with pH 7.4 representing normal tissue and pH 6.5 and pH 6.9 representing tumor tissue. Lower intracellular uptake and, hence lower cytotoxicity of doxorubicin at slightly acidic pH were previously reported [22]. We also found the pH dependent cytotoxicity of free THP as similar to doxorubicin (Fig. 3C) and likewise cellular uptake (data not shown). Free THP had a lower cytotoxicity when HeLa cells were cultured at the lower pH value, whereas PHPMA-hyd-THP demonstrated a somewhat higher cytotoxicity at lower pH values (pH 6.5 and 6.9) than at pH 7.4 (Fig. 3C and D). These results suggest that PHPMA-hyd-THP was more toxic in the tumor tissue environment than in the normal tissue environment, which indicates a tumor-selective toxicity, as well as tumor-selective accumulation, as described later.

Another issue is whether the cleavage and release of free drugs from the polymer conjugate would take place inside or outside the cells. Malugin et al. previously reported that noncleavable HPMA conjugated with doxorubicin (HPMA-GG-DOX) showed a much lower cytotoxicity (10,000 times lower) compared with free doxorubicin [23]. HPMA-GFLG-DOX, in which doxorubicin was conjugated to polymeric HPMA by a cathepsin B-cleavable peptide linkage (glycylphenylalanylleucylglycine, GFLG), had a 10 times higher cytotoxicity than HPMA-GG-DOX, a noncleavable conjugate, in a study of in vitro cytotoxic activity [23]. The GFLG linkage can be cleaved by cathepsin B (a lysosomal enzyme) or by a similar protease in some cancer cells, with the free doxorubicin being released in the lysosomal compartment, diffusing into the cytoplasm and nucleus, and then exerting pharmacological activity. This finding indicates that the liberation of free doxorubicin is critical for its pharmacological action.

Another biodegradable linkage is the hydrazone bond, which is utilized to liberate free drugs in acidic milieus such as lysosomal and cancer environments [13,14]. HPMA-hyd-DOX (polymeric HPMA conjugated to doxorubicin via a hydrazone bond) showed a far greater cytotoxicity (100 times more) than that of HPMA-GFLG-DOX [13]. This big difference in cytotoxicity between HPMA-hyd-DOX and HPMA-GFLG-DOX may indicate that part of the hydrazone bond is cleaved outside the cells, because intracellular uptake of HPMA macromolecules is much slower than that of free drugs. We therefore determined the amount of THP in PHPMA-hyd-THP-treated and free THP-treated cells. We treated HeLa cells with PHPMA-hyd-THP and quantified the amounts of the intracellular drugs, i.e., free THP and total THP, by using HPLC. Most of the drugs existed as free THP, not as PHPMA-hyd-THP, in cancer cells (Fig. 3E). Furthermore, treatment with bafilomycin A1, a lysosomal V-ATPase inhibitor, did not increase the PHPMA-hyd-THP ratio inside the cells (Fig. 3E). These results indicate that PHPMA-hyd-THP was mostly cleaved outside the cells, and then the released THP was internalized by the cells.

3.4. In vivo antitumor activity of THP-polymer conjugates

We next investigated in vivo antitumor activity of PHPMA-hyd-THP against mouse sarcoma S-180. Two THP-equivalent doses of free THP and PHPMA-hyd-THP at 5 mg/kg and 15 mg of THP per kg equivalent were administered only once via the tail vein at 10 days after tumor cell inoculation, when the tumor diameter was 5–8 mm. Free THP was effective at both 5 and 15 mg/kg doses in mice and suppressed tumor growth throughout the experimental period (3 months); however, administration of free THP at 15 mg/kg to tumor-bearing mice caused two of five mice to die of toxicity (Fig. 4), and the body weight of the mice was markedly reduced (Fig. 4C). PHPMA-hyd-THP was more effective than free THP administered at 5 and 15 mg/kg; most mice were completely cured as of day 90. The more important effects noted in this group included no body weight loss or acute death, so that all tumor-bearing mice treated with PHPMA-hyd-THP had survived by day 90, whereas the group treated with free THP at 15 mg/kg demonstrated only 40% survival (Fig. 4D).

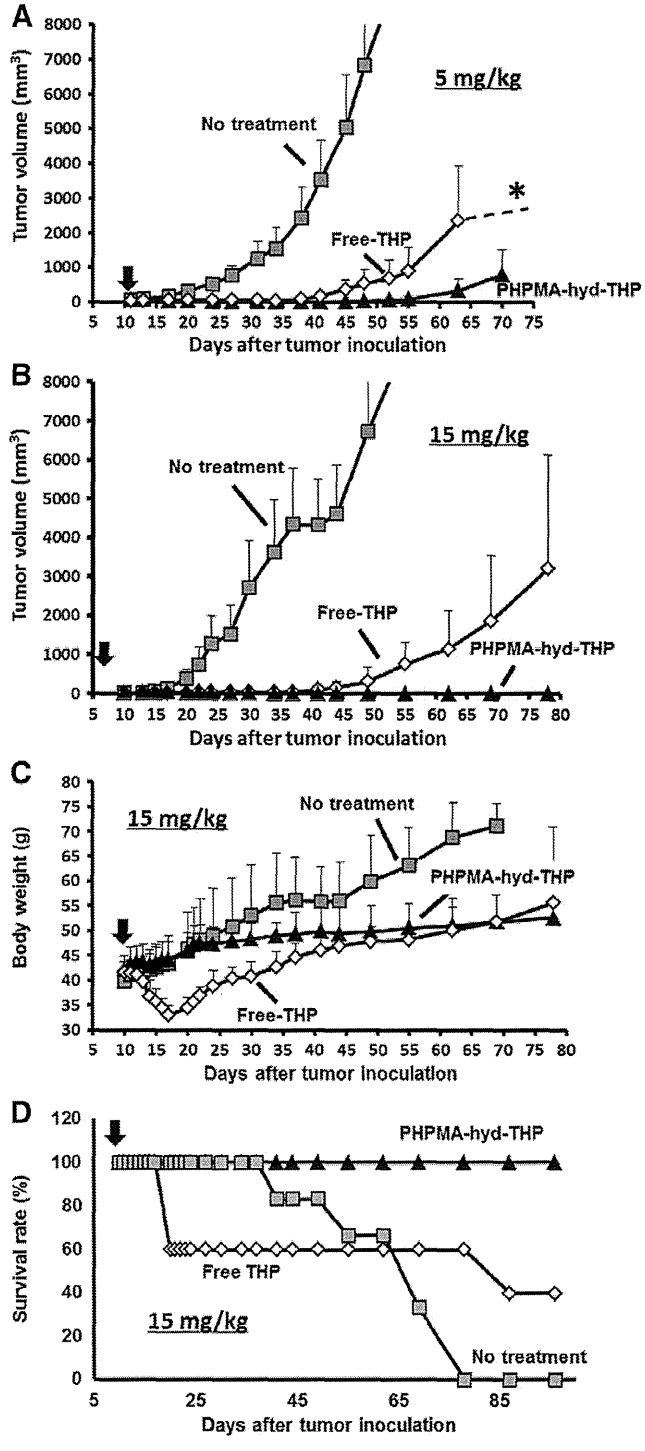

Fig. 4. Antitumor activity of PHPMA-hyd-THP in vivo. (A) and (B) PHPMA-hyd-THP or free THP was administered once at (A) 5 mg/kg or (B) 15 mg of THP per kg equivalent into S-180 tumor-bearing mice. (C) Body weight change and (D) survival rate after administration of 15 mg of THP per kg equivalent into S-180 tumor-bearing mice. Values are means + s.e. (n = 5–6). *One mouse out of five with largest tumor died, tumors of remaining mice continue to grow.

3.5. Tissue distribution of THP-polymer conjugates at different time points and release of free THP in tumor tissue

We also investigated the body distribution of free THP and PHPMA-hyd-THP in S-180 tumor-bearing mice. At 10 days after tumor cell inoculation at dorsal skin, 10 mg of THP per kg equivalent of free THP or its polymer conjugate was administered once i.v. to S-180 tumor-bearing mice. After free THP was injected, it disappeared rapidly from the systemic circulation, within 5 h, and most free THP was found in the spleen, liver, intestine, and lung, only at 5 h (Fig. 5A). In contrast, after PHPMA-hyd-THP was injected i.v., it was found predominantly in the systemic circulation at 5 h, and marked accumulation in the tumor could be seen as well (Fig. 5B), with accumulation in tumor tissue being 4–20 times higher than accumulation in normal tissue, except for the spleen, at 24, 48, and 72 h after drug administration. As a more interesting finding, the amount of THP released from PHPMA-hyd-THP in the tumor tissue was highest at 24 h (Fig. 5C), whereas the total THP amount decreased gradually in tumor tissue (cf. 5 h vs. 24 h) (Fig. 5B and C). Furthermore, the content of free THP in the tumor tissue was far higher than that in any normal tissues after 24, 48, and 72 h (Fig. 5C). This tumor selective accumulation of released free THP can be explained as follows. One is tumor selective accumulation and retention of PHPMA-hyd-THP by EPR effect, and second is efficient release of free THP in the acidic tumor environment. More interesting is that ratio of released free THP to total THP in the tumor became higher than that of normal tissue as time progressed (Fig. 5D). This result suggests that PHPMA-hyd-THP selectively released free THP in acidic environment of the tumor, as shown in Fig. 3A. THP, but not DOX, is transported into the tumor cells by concentrative nucleoside transporter 2 (CNT2) [24]. CNT2 is highly expressed in the tumor cells, thus released free THP would be incorporated quickly into the cancer cells rather than diffusing back to the systemic circulation, this also might be one of the reasons why free THP was accumulated remarkably in the tumor tissue upon administration of PHPMA-hyd-THP [25]. CNT2 is also highly expressed in the spleen, thymus, and part of the intestine; furthermore it might be due to the higher blood flow in the spleen, thus THP tends to accumulate in the spleen, as seen by administration of unconjugated THP (Fig. 5A). PHPMA-hyd-THP is relatively stable in the neutral pH, such as systemic circulation and normal tissues; however release of free THP was gradually occurred even in the systemic circulation. Thus released free THP from polymer conjugates in the systemic circulation would be captured by the spleen; resulting in higher free THP level in the spleen (Fig. 5B). Because free THP is the active form of the drug for cytotoxic effects, a high level of released free THP in the tumor tissue is most desirable for superior antitumor activity. As seen in Fig. 4A and B, PHPMA-hyd-THP indeed had much better antitumor effects than did free THP.

4. Conclusions

Most cytotoxic antitumor drugs exert their effects by interacting with molecular targets such as DNA, DNA topoisomerase, and tubulin. Some molecular targets, such as human epidermal growth factor receptor 2 (HER2) and vascular endothelial growth factor, are located on the cell surface; however, many targets exist inside the cells. Therefore, many antitumor drugs must be internalized by the cells for their effective interaction to target molecules. With regard to interaction with the cell surface, many macromolecular drugs are masked or modified by biocompatible polymers such as PEG, and as a result this modification will suppress interaction with the cell surface target and then intracellular uptake will be impeded [20]. Release of low-Mw antitumor drugs from micelles or carrier macromolecules in the tumor tissue will thus have a great impact on cytotoxicity. In this study, we prepared and investigated an acid-cleavable linkage, the hydrazone bond, in biological systems to study the release of free THP from the carrier polymer (HPMA copolymer) in weakly acidic pH, which represented the pH

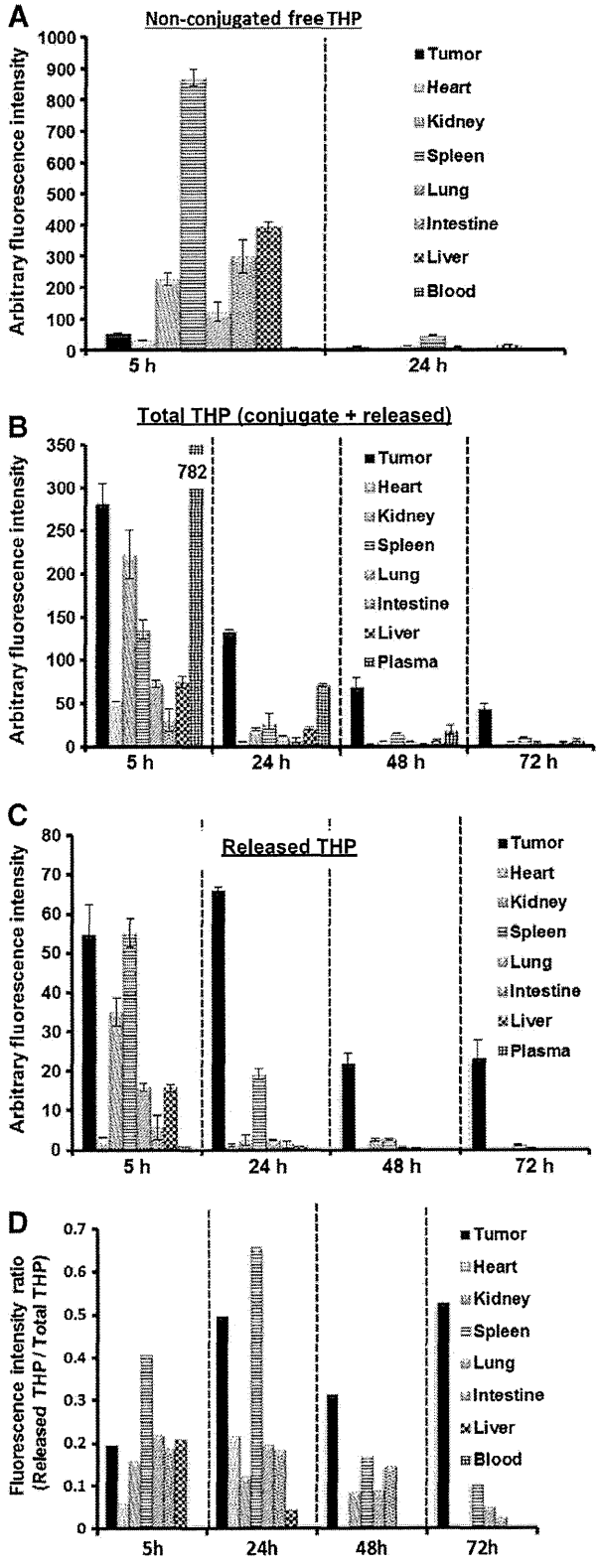

Fig. 5. Body distribution of PHPMA-hyd-THP. (A) Free THP was administered at 10 mg of THP per kg equivalent. (B) and (C) Profile of PHPMA-hyd-THP administered at 10 mg of THP per kg equivalent into S-180 tumor-bearing mice. At the indicated time periods, mice were anesthetized and tissues were collected. (B) Total THP content and (C) released free THP content in each tissue were measured by means of HPLC. See details in Materials and methods. Values are means ± s.e. (n = 3) (D) Ratio of free THP to total THP in each tissue. The fluorescence intensity of the free THP was divided by the fluorescence intensity of the total THP.

environment of tumor tissue in general, as we attempted to achieve drug release in a tumor-selective manner. As expected, PHPMA-hyd-THP showed superior tumor accumulation because of the EPR effect, the first tumor-selective mechanism, and then it released free THP in the tumor as the second tumor-selective mechanism. Our results demonstrated marked antitumor effects without notable adverse effects, even after one intravenous injection. Thus, the PHPMA-hyd-THP conjugate seems to offer a great benefit for highly tumor-selective solid tumor chemotherapy.

Acknowledgments

The authors acknowledge support from the Ministry of Health, Labour and Welfare (MLHW) 2007–2013, the Japan for Cancer Specialty Grant to Hiroshi Maeda (2011–2014) and from the Matching Fund Subsidy for Private Universities from the Ministry of Education, Culture, Sports, Science and Technology (MECSST), Japan. We also acknowledge the support with a grant Praemium Academiae from Academy of Sciences of the Czech Republic, to Karel Ulbrich.

References

[1] Y. Matsumura, H. Maeda, A new concept for macromolecular therapeutics in cancer chemotherapy: mechanism of tumoritropic accumulation of proteins and the antitumor agent smancs, Cancer Res. 46 (12 Pt 1) (1986) 6387–6392.
[2] J. Fang, H. Nakamura, H. Maeda, The EPR effect: unique features of tumor blood vessels for drug delivery, factors involved, and limitations and augmentation of the effect, Adv. Drug Deliv. Rev. 63 (3) (2011) 136–151.
[3] H. Maeda, Vascular permeability in cancer and infection as related to macromolecular drug delivery, with emphasis on the EPR effect for tumor-selective drug targeting, Proc. Jpn. Acad. Ser. B Phys. Biol. Sci. 88 (3) (2012) 53–71.
[4] T. Lammers, Drug delivery research in Europe, J. Control. Release 161 (2) (2012) 151.
[5] V. Torchilin, Tumor delivery of macromolecular drugs based on the EPR effect, Adv. Drug Deliv. Rev. 63 (3) (2011) 131–135.
[6] Y. Noguchi, J. Wu, R. Duncan, J. Strohalm, K. Ulbrich, T. Akaike, H. Maeda, Early phase tumor accumulation of macromolecules: a great difference in clearance rate between tumor and normal tissues, Jpn. J. Cancer Res. 89 (3) (1998) 307–314.
[7] W.C. Zamboni, Liposomal, nanoparticle, and conjugated formulations of anticancer agents, Clin. Cancer Res. 11 (23) (2005) 8230–8234.
[8] E. Fleige, M.A. Quadir, R. Haag, Stimuli-responsive polymeric nanocarriers for the controlled transport of active compounds: concepts and applications, Adv. Drug Deliv. Rev. 64 (9) (2012) 866–884.
[9] W.C. Zamboni, Concept and clinical evaluation of carrier-mediated anticancer agents, Oncologist 13 (3) (2008) 248–260.
[10] M.J. Vicent, R. Tomlinson, S. Brocchini, R. Duncan, Polyacetal-diethylstilboestrol: a polymeric drug designed for pH-triggered activation, J. Drug Target. 12 (8) (2004) 491–501.
[11] Y. Bae, N. Nishiyama, S. Fukushima, H. Koyama, M. Yasuhiro, K. Kataoka, Preparation and biological characterization of polymeric micelle drug carriers with intracellular pH-triggered drug release property: tumor permeability, controlled subcellular drug distribution, and enhanced *in vivo* antitumor efficacy, Bioconjug. Chem. 16 (1) (2005) 122–130.
[12] Y. Bae, N. Nishiyama, K. Kataoka, *In vivo* antitumor activity of the folate-conjugated pH-sensitive polymeric micelle selectively releasing adriamycin in the intracellular acidic compartments, Bioconjug. Chem. 18 (4) (2007) 1131–1139.
[13] B. Rihova, T. Etrych, M. Pechar, M. Jelinkova, M. Stastny, O. Hovorka, M. Kovar, K. Ulbrich, Doxorubicin bound to a HPMA copolymer carrier through hydrazone bond is effective also in a cancer cell line with a limited content of lysosomes, J. Control. Release 74 (1–3) (2001) 225–232.
[14] S.O. Doronina, B.E. Toki, M.Y. Torgov, B.A. Mendelsohn, C.G. Cerveny, D.F. Chace, R.L. DeBlanc, R.P. Gearing, T.D. Bovee, C.B. Siegall, J.A. Francisco, A.F. Wahl, D.L. Meyer, P.D. Senter, Development of potent monoclonal antibody auristatin conjugates for cancer therapy, Nat. Biotechnol. 21 (7) (2003) 778–784.
[15] T. Etrych, M. Jelinkova, B. Rihova, K. Ulbrich, New HPMA copolymers containing doxorubicin bound via pH-sensitive linkage: synthesis and preliminary *in vitro* and *in vivo* biological properties, J. Control. Release 73 (1) (2001) 89–102.
[16] H.S. Yoo, E.A. Lee, T.G. Park, Doxorubicin-conjugated biodegradable polymeric micelles having acid-cleavable linkages, J. Control. Release 82 (1) (2002) 17–27.
[17] J. Yang, H. Chen, I.R. Vlahov, J.X. Cheng, P.S. Low, Characterization of the pH of folate receptor-containing endosomes and the rate of hydrolysis of internalized acid-labile folate-drug conjugates, J. Pharmacol. Exp. Ther. 321 (2) (2007) 462–468.
[18] H. Umezawa, Y. Takahashi, M. Kinoshita, H. Naganawa, T. Masuda, M. Ishizuka, K. Tatsuta, T. Takeuchi, Tetrahydropyranyl derivatives of daunomycin and adriamycin, J. Antibiot (Tokyo) 32 (10) (1979) 1082–1084.
[19] S. Kunimoto, K. Miura, Y. Takahashi, T. Takeuchi, H. Umezawa, Rapid uptake by cultured tumor cells and intracellular behavior of 4′-O-tetrahydropyranyladriamycin, J. Antibiot (Tokyo) 36 (3) (1983) 312–317.
[20] H. Hatakeyama, H. Akita, K. Kogure, M. Oishi, Y. Nagasaki, Y. Kihira, M. Ueno, H. Kobayashi, H. Kikuchi, H. Harashima, Development of a novel systemic gene delivery system for cancer therapy with a tumor-specific cleavable PEG-lipid, Gene Ther. 14 (1) (2007) 68–77.
[21] T. Masuda, H. Akita, K. Niikura, T. Nishio, M. Ukawa, K. Enoto, R. Danev, K. Nagayama, K. Ijiro, H. Harashima, Envelope-type lipid nanoparticles incorporating a short PEG-lipid conjugate for improved control of intracellular trafficking and transgene transcription, Biomaterials 30 (27) (2009) 4806–4814.
[22] L.E. Gerweck, S.V. Kozin, S.J. Stocks, The pH partition theory predicts the accumulation and toxicity of doxorubicin in normal and low-pH-adapted cells, Br. J. Cancer 79 (5–6) (1999) 838–842.
[23] A. Malugin, P. Kopeckova, J. Kopecek, Liberation of doxorubicin from HPMA copolymer conjugate is essential for the induction of cell cycle arrest and nuclear fragmentation in ovarian carcinoma cells, J. Control. Release 124 (1–2) (2007) 6–10.
[24] K. Nagai, K. Nagasawa, A. Ishimoto, S. Fujimoto, Pirarubicin is taken up by a uridine-transportable sodium-dependent concentrative nucleoside transporter in Ehrlich ascites carcinoma cells, Cancer Chemother. Pharmacol. 51 (6) (2003) 512–518.
[25] H. Lu, C. Chen, C. Klaassen, Tissue distribution of concentrative and equilibrative nucleoside transporters in male and female rats and mice, Drug Metab. Dispos. 32 (12) (2004) 1455–1461.

Identification of heat shock protein 32 (Hsp32) as a novel target in acute lymphoblastic leukemia

Sabine Cerny-Reiterer[1,2], Renata A. Meyer[2], Harald Herrmann[1,2], Barbara Peter[1,2], Karoline V. Gleixner[2], Gabriele Stefanzl[2], Emir Hadzijusufovic[1,2,3], Winfried F. Pickl[4], Wolfgang R. Sperr[2], Junia V. Melo[5], Hiroshi Maeda[6], Ulrich Jäger[2], Peter Valent[1,2]

[1] Ludwig Boltzmann Cluster Oncology, Medical University of Vienna, Austria;

[2] Department of Internal Medicine I, Division of Hematology & Hemostaseology, Medical University of Vienna, Austria;

[3] Department of Companion Animals and Horses, Clinic for Internal Medicine and Infectious Diseases, University of Veterinary Medicine Vienna, Vienna, Austria;

[4] Institute of Immunology, Medical University of Vienna, Austria;

[5] Department of Haematology Centre for Cancer Biology, Adelaide, Australia; and

[6] Laboratory of Microbiology and Oncology, Faculty of Pharmaceutical Sciences, Sojo University, Kumamoto and BioDynamics, Research Laboratory, Kumamoto, Japan

Correspondence to: *Peter Valent,* ***email:*** *peter.valent@meduniwien.ac.at*

Keywords: ALL, imatinib-resistance, Hsp32, HO-1, targeting

Received: *February 13, 2014* ***Accepted:*** *March 2, 2014* ***Published:*** *March 4, 2014*

ABSTRACT:

Heat shock proteins (Hsp) are increasingly employed as therapeutic targets in oncology. We have shown that Hsp32, also known as heme oxygenase-1 (HO-1), serves as survival factor and potential target in Ph$^+$ chronic myeloid leukemia. We here report that primary cells and cell lines derived from patients with acute lymphoblastic leukemia (ALL) express Hsp32 mRNA and the Hsp32 protein in a constitutive manner. Highly enriched CD34$^+$/CD38$^-$ ALL stem cells also expressed Hsp32. Two Hsp32-targeting drugs, pegylated zinc protoporphyrine (PEG-ZnPP) and styrene maleic acid-micelle-encapsulated ZnPP (SMA-ZnPP), induced apoptosis and growth arrest in the BCR/ABL1$^+$ cell lines, in Ph$^-$ lymphoblastic cell lines and in primary Ph$^+$ and Ph$^-$ ALL cells. The effects of PEG-ZnPP and SMA-ZnPP on growth of leukemic cells were dose-dependent. In Ph$^+$ ALL, major growth-inhibitory effects of the Hsp32-targeting drugs were observed in imatinib-sensitive and imatinib-resistant cells. Hsp32-targeting drugs were found to synergize with imatinib, nilotinib, and bendamustine in producing growth inhibition and apoptosis in Ph$^+$ ALL cells. A siRNA against Hsp32 was found to inhibit growth and survival of ALL cells and to synergize with imatinib in suppressing the growth of ALL cells. In conclusion, Hsp32 is an essential survival factor and potential new target in ALL.

INTRODUCTION

Acute lymphoblastic leukemia (ALL) is a life-threatening neoplasm characterized by uncontrolled growth and leukemic expansion of immature lymphoblastic progenitor cells [1-4]. The prognosis and outcome in ALL depend on age, molecular defects and response to therapy [1-6]. In about 30% of all adult patients, leukemic cells display the Philadelphia chromosome (Ph) and the related fusion gene, *BCR/ABL1* [1-6]. In the 'pre-imatinib-era', these patients had an extremely poor prognosis compared to patients with Ph$^-$ ALL [5,6]. Since then the prognosis of patients with BCR/ABL1$^+$ ALL has improved, which is largely attributable to the effects of novel BCR/ABL1-targeting drugs [7-12]. In fact, the BCR/ABL1 tyrosine kinase inhibitor (TKI) imatinib is effective in most patients with newly diagnosed Ph$^+$ ALL, and sometimes even in patients with chemotherapy-resistant or relapsed Ph$^+$ ALL,

especially when applied in combination with conventional chemotherapy [7-13]. Second- and third generation BCR/ABL1 blockers are also effective in patients with Ph^+ ALL [14].

However, not all patients with Ph^+ ALL respond to standard treatment and TKI. Therefore, depending on age, risk factors, and availability of a donor, stem cell transplantation (SCT) is recommended for patients with drug-resistant and high risk ALL [15-18]. In these patients, the overall treatment plan often combines chemotherapy, SCT and BCR/ABL1-targeting drugs [17]. However, despite SCT and the availability of novel targeted drugs, not all patients with Ph^+ ALL can be cured. Therefore, current research focuses on identifying new targets and drugs that can be employed in these patients and may improve outcome and survival in ALL the future.

One class of interesting new targets in oncology are heat shock proteins (Hsp). These proteins often act as survival factors and are expressed in neoplastic cells in a constitutive manner [19]. Heat shock protein 32 (Hsp32), also known as heme oxygenase-1 (HO-1), is a stress-related cytoprotective molecule that is expressed in normal and neoplastic cells, including myeloid leukemias [20-28]. In neoplastic cells, Hsp32 is considered to play a major role as an essential survival factor [22-29]. We have recently shown that Hsp32 (HO-1) is expressed in leukemic cells in Ph^+ chronic myeloid leukemia (CML) and that Hsp32-targeting drugs produce growth arrest and apoptosis in leukemic cells [28,29].

In the present study, we show that Hsp32 is expressed in leukemic cells in Ph^+ and Ph^- ALL, and that pharmacologic inhibitors of Hsp32 suppress the growth of imatinib-sensitive as well as imatinib-resistant ALL cells. Moreover, we show that drug combinations consisting of Hsp32 inhibitors and either BCR/ABL1 TKI or bendamustin, can produce synergistic growth-inhibitory effects in imatinib-resistant ALL cells.

RESULTS

ALL cells express Hsp32 mRNA and the Hsp32 protein

As assessed by qPCR, primary ALL cells as well as the ALL cell lines tested were found to express Hsp32 mRNA (Figure 1A, Tables 1 and 2). Hsp32 transcripts were present in Ph^+ ALL cells as well as in Ph^- ALL cells (Figure 1A). Hemin was found to promote expression of Hsp23 mRNA in all ALL samples tested (Figure 1A). We were also able to show that ALL cells display the Hsp32 protein. Expression of the Hsp32 protein was demonstrable by immunocytochemistry (Figure 1B) as well as by Western blotting (Figure 1C), and hemin was found to upregulate expression of the Hsp32 protein in ALL cells (Figure 1B and 1C). Since leukemic stem cells are considered a major target of therapy, we were also interested to know whether CD34+/CD38− stem cells in ALL express Hsp32. In these experiments, we were able to show that highly enriched (sorted) $CD34^+/CD38^-$ ALL stem cells as well as $CD34^+/CD38^+$ progenitor cells express Hsp32 mRNA in patients with Ph^+ ALL and patients with Ph^- ALL (Figure 1D).

BCR/ABL1-targeting drugs down regulate expression of Hsp32 in ALL cells

We have recently shown that expression of Hsp32 in CML cells is triggered by BCR/ABL1 [28,29]. Therefore, we were interested to learn whether BCR/ABL1-targeting drugs would alter expression of Hsp32 in Ph^+ ALL cells. As assessed by qPCR, imatinib was found to down regulate expression of Hsp32 mRNA in the Ph^+ ALL cell lines TOM-1 and NALM-1 (Figure 2A). In contrast, imatinib did not suppress expression of Hsp32 mRNA in the Ph^- ALL cell lines tested (Figure 2A). These data suggest that BCR/ABL1 is involved in the expression of Hsp32 in Ph^+ ALL, whereas in Ph^- ALL, other mechanisms contribute to Hsp32 expression.

Depletion of Hsp32 leads to apoptosis and growth arrest in ALL cells

Hsp32 is a well-known survival factor that counteracts apoptosis in various cell types. To investigate the functional role of Hsp32 in ALL cells, expression of Hsp32 was specifically silenced by siRNA in the Ph^+ ALL cell lines TOM-1 and NALM-1 and in the Ph^- cell line Raji. The siRNA-induced knockdown of Hsp32 was found to be associated with a significant decrease in cell viability due to an increase of apoptotic cells (Figure 2B). A control siRNA (against Luc) showed no substantial effect on expression of Hsp32 and no effect on survival (apoptosis) of ALL cells (Figure 2B). As expected, the siRNA-induced knock-down of Hsp32 also induced growth arrest in the ALL cell lines tested (Figure 2B).

Effects of pharmacologic inhibitors of Hsp32 on growth of ALL cell lines

To evaluate the role of Hsp32 as a potential therapeutic target in ALL cells, two water-soluble pharmacologic inhibitors were applied, SMA-ZnPP and PEG-ZnPP. As assessed by ^{3}H-thymidine uptake, both Hsp32-targeting drugs were found to inhibit the proliferation of Ph^+ and Ph^- ALL cells (primary cells and cell lines) after 48 hours of incubation (Figure 2C and Figure 2D). The effects of both drugs on growth of ALL cells were dose-dependent, with comparable IC50 values

Table 1: Patients´ characteristics, detection of Hsp32 in leukemic cells, and response to SMA-ZnPP and PEG-ZnPP

Patient No.(#)	Gender	Age (year)	Diagnosis	BCR/ ABL1	WBC (G/L)	Hb (g/dL)	Plt (G/L)	Cytogenetics	ICC Hsp32	PCR Hsp32	SMA ZnPP IC50	PEG ZnPP IC50
#1	f	33	c-ALL	-	52.1	12.6	139	46,XX	+	+	20 μM	20 μM
#2	m	73	pre-B-ALL	p210	140	10	19	47,XY,t(9;22) (q34;q11)+20	+	+	5 μM	20 μM
#3	m	39	c-ALL	p190	61.6	9.4	56	46,XY, t(9;22) (q34;q11)	+	+	1 μM	20 μM
#4	f	20	pre-B-ALL	-	14.6	8.7	29	46,XX, complex	+	+	5 μM	n.t.
#5	f	35	c-ALL	p190	24.72	13.1	177	53,XX,t(9;22) (q34;q11, complex	+	+	1 μM	5 μM
#6	f	65	pre-B-ALL	-	170	9.1	111	46,XX,t(2;5), t(4;11)	+	+	n.t.	n.t.
#7	f	21	c-ALL	-	568	7.1	75	46,XX	+	+	1 μM	5 μM
#8	m	17	pre-T-ALL	-	4.2	8.1	16	47,XY, del(13), +19	+	+	n.t.	n.t.
#9	f	56	pre-B-ALL	p190	2.3	7.4	86	46,XX, t(9;22) (q34;q11)	+	+	n.t.	n.t.
#10	f	64	biphenotypic AL	p210	53.2	10.5	91	46,XX, t(9;22) (q34;q11)	+	+	n.t	n.t.
#11	f	71	T-ALL	-	9.3	5.5	30	46,XX, complex	+	+	10 μM	0.5 μM
#12	m	60	pre-B-ALL	-	37.6	18.5	77	46,XY, t(1;19),del(13)	+	+	5 μM	10 μM
#13	f	55	c-ALL	p190	71.29	13.7	73	46, XX, t(9;22) (q34;q11)	+	+	n.t.	n.t.
#14	m	17	pre-B-ALL	-	19.74	3.9	114	46,XY,del(9) (q21), idem+8	+	+	n.t.	n.t.
#15	m	60	c-ALL	p210	2.31	9	209	46,XY, t(9;22) (q34;q11), complex	+	+	0.5 μM	0.5 μM
#16	f	45	T-ALL	-	92.02	9	15	46,XX	+	+	n.t	n.t.
#17	f	35	c-ALL*	p210*	32.97	9.7	172	46,XX, t(9;22) (q34;q11)	+	+	5 μM	5 μM
#18	f	35	pre-B-ALL	-	155.26	8.6	52	46,XX,t(19;11), complex	+	+	n.t.	n.t.
#19	f	37	pre-B-ALL	p190	4.4	7.6	3	46,XX, t(9;22) (q34;q11)	+	+	n.t.	n.t.
#20	m	38	T-ALL	-	26.8	8.9	52	46,XY[13]/47, XY, del(13)(q14), der(14)x2, add(16)(q24)[2]	+	+	n.t.	n.t.
#21	f	57	pre-B-ALL	-	10.31	9.7	141	46,XX	n.t	n.t.	1 μM	5 μM
#22	m	21	biphenotypic AL	-	31.73	11.3	75	46,XY, t(2;14)	n.t.	n.t.	1 μM	20 μM
#23	m	63	CML, BP-Ly*	p210*	69.99	12.1	121	46,XY, t(9;22) (q34;q11), complex	n.t	n.t.	10 μM	1 μM
#24	f	22	relapsed pre-B-ALL	-	17.65	9.6	24	47,XX, t(14;14), complex	+	+	1 μM	n.t.
#25	m	72	c-ALL	p210	106.01	10.1	73	46, XY, t(9;22) (q34;q11)	n.t.	+	n.t.	n.t.
#26	f	32	pre-B-ALL	-	117.88	8.9	69	46,XX,del(9) (p13)	n.t.	+	n.t.	n.t.

*In these patients, imatinib resistance developed during the course of disease; in patient #23, a BCR/ABL1 T315I mutation was detected. For evaluation of proliferation, ALL cells were cultured in control medium or in various concentrations of Hsp32-inhibitors for 48 hours. Thereafter, 3H-thymidine-uptake was measured and IC50 values (μM) determined. Abbreviations: WBC, white blood cell count; Hb, hemoglobin; Plt, platelet count; ICC, immunocytochemistry; n.t., not tested; p210, BCR/ABL1 major breakpoint; p190, BCR/ABL1 minor breakpoint.

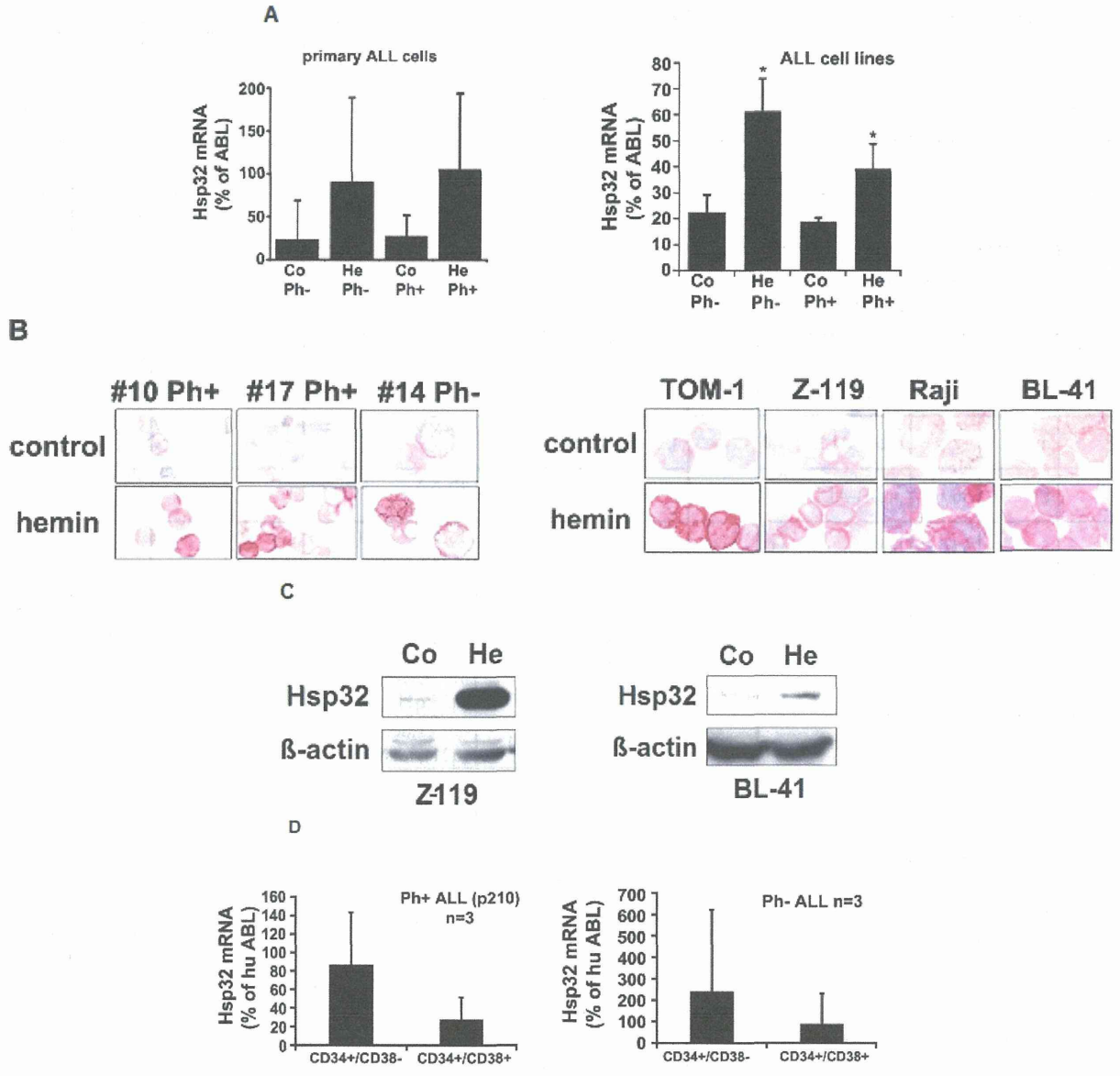

Figure 1:Expression of Hsp32 in ALL cells. A: Primary ALL cells (left panel) and cell lines (right panel) were subjected to RNA isolation and RT-PCR using primers specific for Hsp32 and human ABL (control) as described in the text. Before RNA was isolated, cells were cultured in control medium (Co) or in medium containing 10 μM hemin (He) at 37°C for 8 hours. Expression of Hsp32 mRNA and ABL mRNA was determined by qPCR. The left panel shows data obtained with primary ALL cells (7 Ph^+ donors and 10 Ph^- donors) and the right panel shows data obtained with Ph^+ and Ph^- cell lines (Ph^+: BV-173, NALM-1, TOM-1, Z-119, Ph^-: Raji, Ramos, REH, BL-41). Hsp32 mRNA levels are expressed as percentage of ABL mRNA levels and represent the mean±S.D. from all donors or cell lines. Asterisk: $p<0.05$. B: Immunocytochemical detection of the Hsp32 protein in primary ALL cells (left panel, Ph^+ patients #10 and #17; and Ph^- patient #14 from Table 1) and cell lines (right panel) after incubation in control medium or hemin (10 μM) at 37°C for 8 hours. After incubation, cells were spun on cytospin slides and stained with an antibody against Hsp32 as described in the text. Images were taken using an Olympus DP21 camera connected to an Olympus BX50F4 microscope equipped with 100x/1.35 UPlan-Apo objective lense (Olympus, Hamburg, Germany). Figures were prepared using Adobe Photoshop CS2 software version 9.0 (Adobe Systems, San Jose, CA) and processed with PowerPoint software (Microsoft, Redmond, WA). C: Western blot analysis of expression of Hsp32 in Ph^+ cell line Z-119 (left) and Ph^- cell line BL-41 (right). Cells were incubated with control medium (Co) or hemin (10 μM) (He) at 37°C for 8 hours. Then, cells were lysed and lysates subjected to Western blot analysis using an antibody against Hsp32 and an antibody against ß-actin as described in the text. D: Expression of HO-1 mRNA in highly enriched (sorted) $CD34^+/CD38^-$ stem cells and $CD34^+/CD38^+$ progenitor cells obtained from 3 patients with Ph^- ALL (left side) and 3 patients with Ph^+ ALL (p210 right side) as determined by qPCR. Cells were subjected to RNA isolation, cDNA synthesis and qPCR using primers specific for *HO-1* and *ABL*. Results show HO-1 mRNA levels as percent of ABL mRNA levels, and represent the mean±S.D. of 3 independent experiments (3 patients).

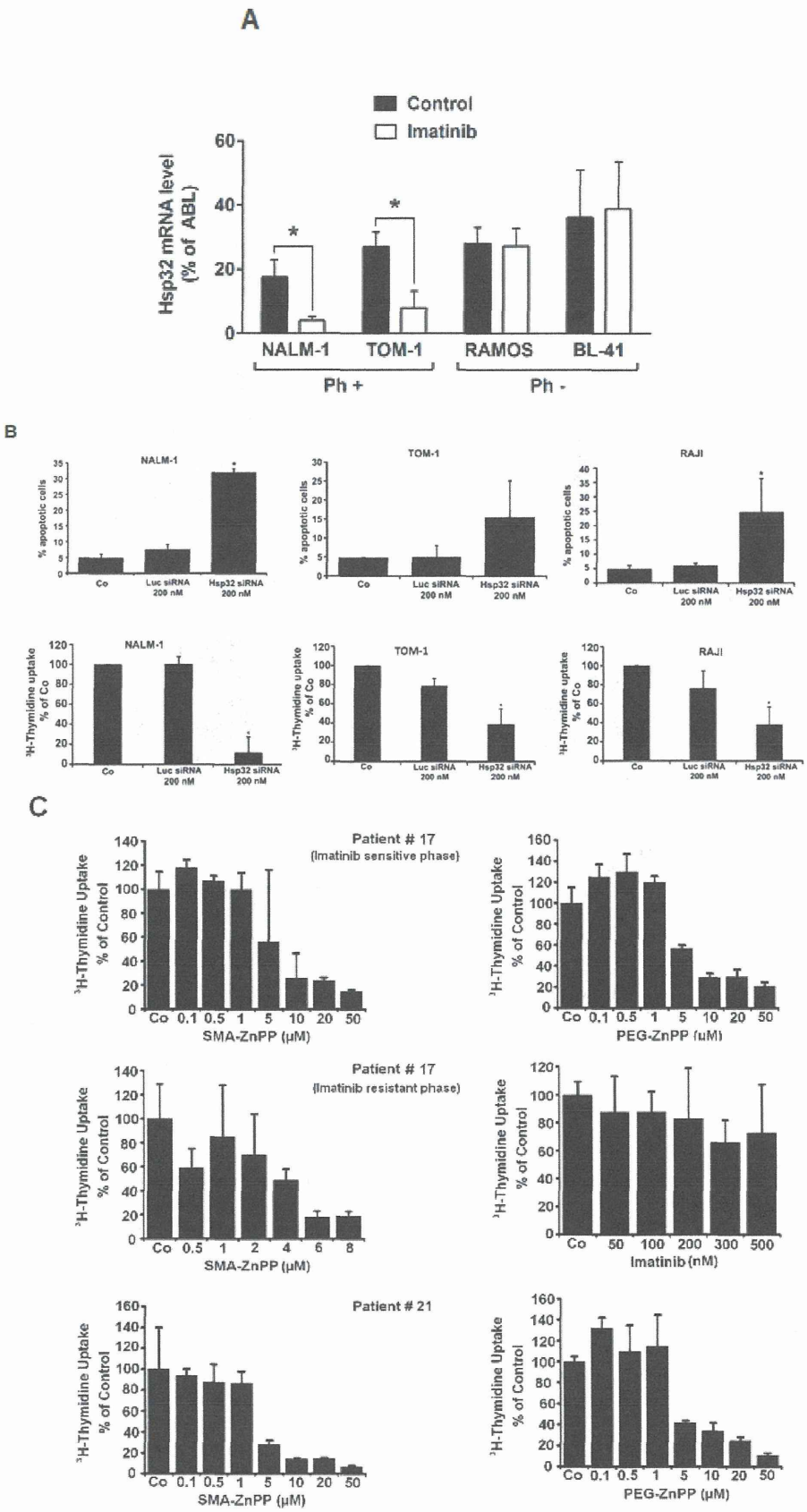
A
Control
Imatinib
Hsp32 mRNA level (% of ABL)
NALM-1
TOM-1
RAMOS
BL-41
Ph +
Ph -
B
NALM-1
TOM-1
RAJI
% apoptotic cells
Co
Luc siRNA 200 nM
Hsp32 siRNA 200 nM
³H-Thymidine uptake % of Co
C
Patient # 17
(Imatinib sensitive phase)
³H-Thymidine Uptake % of Control
SMA-ZnPP (μM)
PEG-ZnPP (μM)
Patient # 17
(Imatinib resistant phase)
Imatinib (nM)
Patient # 21

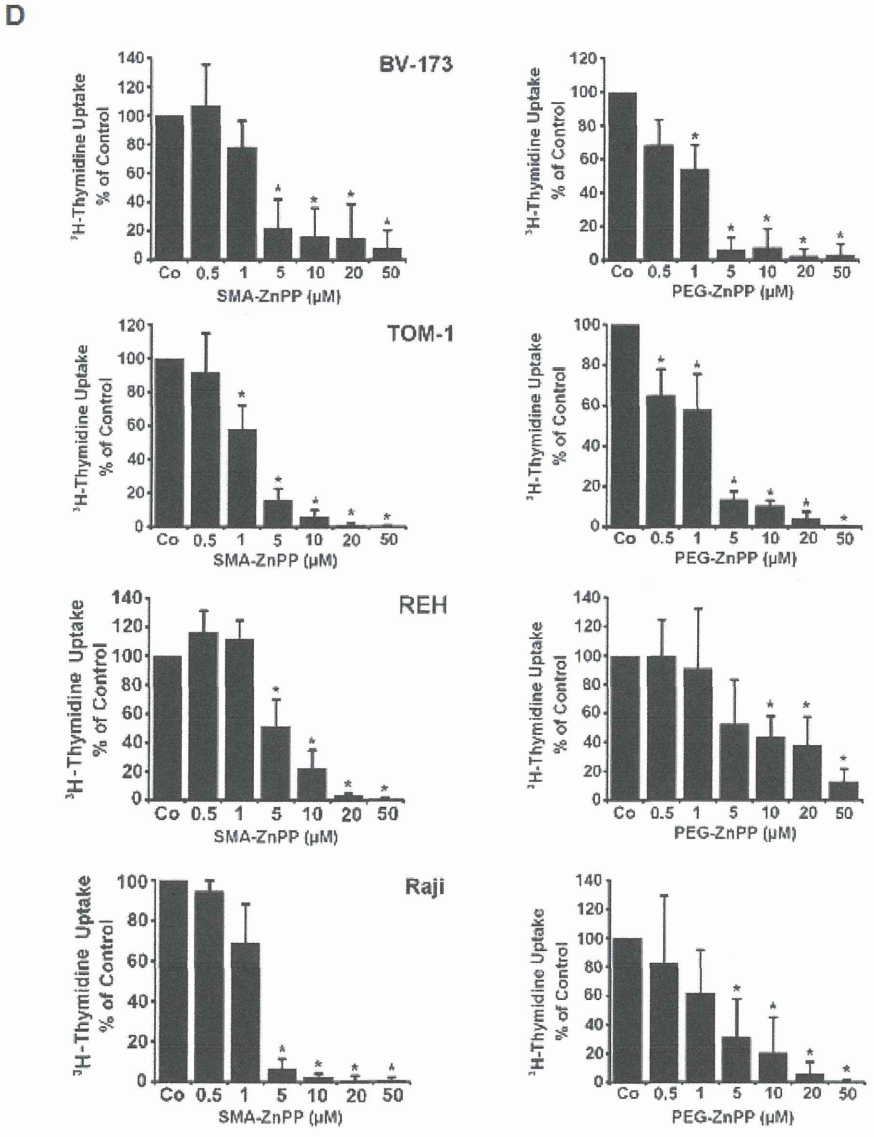

Figure2: Targeting of Hsp32 in ALL cells and functional consequences. A: Effects of BCR/ABL1-targeting drugs on expression of Hsp32 mRNA in leukemic cells. The Ph^+ ALL cell lines NALM-1 and TOM-1 and the Ph^- cell line Ramos and BL-41 were incubated in control medium or imatinib (1 μM) at 37°C for 24 hours. Then, cells were recovered and subjected to RNA isolation and real time PCR using primers specific for Hsp32 and ABL. Results show Hsp32 mRNA expression levels relative to ABL mRNA levels. B: siRNA-induced Hsp32 knockdown in ALL cells is followed by apoptosis. The ALL cell lines NALM-1, TOM-1 and Raji were kept in control medium (Co) or were transfected with a control siRNA against luciferase (Luc siRNA) or siRNA against Hsp32 (200 nM each) as described in the text. After 48 hours, the percentage of apoptotic cells was determined by light microscopy (upper panel). Results represent the mean±S.D. from three independent experiments. Lower panel: ^{3}H-thymidine uptake was measured after transfection with control siRNA or siRNA against Hsp32. Results show the percent of ^{3}H-thymidine uptake compared to control and are expressed as mean±S.D. of triplicates. C,D: PEG-ZnPP and SMA-ZnPP inhibit growth of ALL cells. Primary leukemic cells (C) were obtained from patient #17 at two different time points, i.e. when cells were imatinib-sensitive and later when the patient developed imatinib-resistance, and from patient #21 with Ph^- ALL. Cells were incubated in control medium (Co), various concentrations of PEG-ZnPP or various concentrations of SMA-ZnPP (as indicated) at 37°C for 48 hours. In patient #17, cells were also incubated with imatinib (0.05-0.5 μM) for 48 hours. After incubation, ^{3}H-thymidine uptake was measured. Results show the percentage of ^{3}H-thymidine uptake compared to control and are expressed as mean±S.D. of triplicates. Figure 2D shows result obtained with the Ph^+ ALL cell lines BV-173 and TOM-1 and the Ph^- cell lines REH and Raji. Results show the percentage of ^{3}H-thymidine uptake compared to control and are expressed as mean±S.D. of three independent experiments. Asterisk indicates $p<0.05$.

Table 2: Characterization of cell lines and response to SMA-ZnPP, PEG-ZnPP, and other drugs

Cell Line	Diagnosis	BCR-ABL1	Proliferation Imatinib IC50	ICC Hsp32	PCR Hsp32	Proliferation IC50		Apoptosis EC50	
						SMA-ZnPP IC50	PEG-ZnPP IC50	SMA-ZnPP EC50	PEG-ZnPP EC50
BV-173	B-ALL	p210	0.1 μM	+	+	1-5 μM	1-5 μM	5-10 μM	5 μM
NALM-1	CML, lymphoid BP	p210	0.4μM	+	+	1-5 μM	1-5μM	5 μM	n.t.
TOM-1	B-ALL	p190	0.3 μM	+	+	1-5 μM	1-5 μM	10 μM	15-20 μM
Z-119	B-ALL	p190	0.2 μM	+	+	1 μM	1-5 μM	5 μM	10 μM
RAJI	Burkitt lymphoma	-	>1 μM	+	+	5 μM	5 μM	5-10 μM	20 μM
RAMOS	Burkitt lymphoma	-	>1 μM	+	+	5 μM	5 μM	10 μM	20 μM
REH	B-ALL	-	>1 μM	+	+	5 μM	10 μM	5-10 μM	20 μM
BL-41	Burkitt lymphoma	-	>1 μM	+	+	1-5 μM	1-5 μM	1-5 μM	15 μM

CML, chronic myeloid leukemia; BP, blast phase; ALL, acute lymphoblastic leukemia; p210, BCR/ABL1 major breakpoint; p190, BCR/ABL1 minor breakpoint. Immunocytochemical (ICC) analysis of Hsp32 (HO-1) and qPCR analysis of Hsp32 (HO-1) mRNA expression were performed as described in the text. Cell lines were cultured in control medium or in various concentrations of the Hsp32 (HO-1) inhibitors SMA-ZnPP or PEG-ZnPP, or in the presence of various concentrations of the BCR/ABL1 kinase blockers imatinib or nilotinib for 48 hours. Thereafter, proliferation was measured by 3H-thymidine incorporation assay. IC50 values (μM) represent the mean from at least 3 independent experiments. Apoptosis was determined by light microscopy; EC50 values (μM) represent the mean from at least 3 independent experiments. n.t., not tested.

(Tables 1 and 2).

Hsp32-targeting drugs suppress the growth of leukemic cells from patients with imatinib-resistant ALL

In a substantial number of patients with ALL, leukemic cells develop resistance to imatinib. We were therefore interested to know whether Hsp32-targeting drugs can suppress the growth of leukemic cells from patients with imatinib-resistant Ph^+ ALL. In these experiments, SMA-ZnPP and PEG-ZnPP were found to inhibit growth of primary, imatinib-resistant leukemic cells in a dose-dependent manner in all patients examined (Figure 2C, Table 1), including one patient with lymphoid blast phase exhibiting BCR/ABL T315I (Table 1).

The growth-inhibitory effects of PEG-ZnPP and SMA-ZnPP on ALL cells are associated with induction of apoptosis

Hsp32 has been described as a survival factor counteracting apoptosis in various neoplastic cells. We next investigated whether the growth-inhibitory effects of Hsp32 inhibitors (SMA-ZnPP and PEG-ZnPP) are associated with induction of apoptosis in ALL cells. We found that both drugs induce apoptosis in primary ALL cells and in the ALL cell lines tested (Figure 3 and Table 2). The apoptosis-producing effects of SMA-ZnPP and PEG-ZnPP on ALL cells were demonstrable by light microscopy (Figure 3A and 3B) as well as in a Tunel assay (Figure 3C). Furthermore, we were able to show by flow cytometry that SMA-ZnPP induces activation of caspase-3 in ALL cells (Figure 3D). In normal bone marrow cells, neither SMA-ZnPP nor PEG-ZnPP were found to induce apoptosis over the dose-range tested (1-40 μM) confirming previous data [29].

Hsp32-targeting drugs synergize with BCR/ABL1-targeting drugs (imatinib, nilotinib) and with bendamustine in producing growth inhibition in ALL cells

Next, we examined cooperative drug effects on growth and survival (apoptosis) of ALL cells. We found that Hsp32-targeting drugs synergize with BCR/ABL1 TKI and with bendamustin in inducing growth inhibition and apoptosis in ALL cells (Figure 4A-C). To further validate Hsp32 as a potential drug-partner of TKI in ALL cells, we applied siRNA against Hsp32 and measured the proliferation of ALL cells as well as the response to imatinib. In these experiments, suboptimal concentrations of imatinib were applied. As shown in Figure 4D, addition of Hsp32-specific siRNA was found to potentiate the effects of imatinib on both ALL cell lines examined, TOM-1 and NALM-1.